



The systemic complexity of a monogenic disease: the molecular network of spinal muscular atrophy

Ines Tapken,^{1,2,3} Theresa Schweitzer,^{3,4} Martina Paganin,⁵ Tobias Schüning,¹ Nora T. Detering,^{1,2,3} Gaurav Sharma,⁵ Moritz Niesert,⁶ Afshin Saffari,⁶ Daniela Kuhn,^{1,7} Amy Glynn,¹ Federica Cieri,^{8,9} Pamela Santonicola,⁸ Claire Cannet,¹⁰ Florian Gerstner,¹¹ Kiterie M. E. Faller,¹² Yu-Ting Huang,¹² Rashmi Kothary,¹³ Thomas H. Gillingwater,¹² Elia Di Schiavi,⁸ Christian M. Simon,¹¹ Niko Hensel,¹⁴ Andreas Ziegler,⁶ Gabriella Viero,⁵ Andreas Pich,^{3,4} and Peter Claus^{1,2,15}

Monogenic diseases are well-suited paradigms for the causal analysis of disease-driving molecular patterns. Spinal muscular atrophy (SMA) is one such monogenic model, caused by mutation or deletion of the survival of motor neuron 1 (SMN1) gene. Although several functions of the SMN protein have been studied, single functions and pathways alone do not allow the identification of crucial disease-driving molecules.

Here, we analysed the systemic characteristics of SMA, using proteomics, phosphoproteomics, translaticomics and interactomics, from two mouse models with different disease severities and genetics.

This systems approach revealed subnetworks and proteins characterizing commonalities and differences of both models. To link the identified molecular networks with the disease-causing SMN protein, we combined SMN-interactome data with both proteomes, creating a comprehensive representation of SMA. By this approach, disease hubs and bottlenecks between SMN and downstream pathways could be identified.

Linking a disease-causing molecule with widespread molecular dysregulations via multiomics is a concept for analyses of monogenic diseases.

1 SMATHERIA gGmbH—Non-Profit Biomedical Research Institute, Hannover 30625, Germany

2 Center for Systems Neuroscience (ZSN), Hannover 30559, Germany

3 Research Core Unit Proteomics, Hannover Medical School (MHH), Hannover 30625, Germany

4 Institute of Toxicology, Hannover Medical School (MHH), Hannover 30625, Germany

5 CNR Unit, Institute of Biophysics, Trento 38123, Italy

6 Department of Pediatrics I, Center for Pediatrics and Adolescent Medicine, Heidelberg University, Heidelberg 69120, Germany

7 Department of Conservative Dentistry, Periodontology and Preventive Dentistry, Hannover Medical School, Hannover 30625, Germany

8 CNR, Institute of Biosciences and Bioresources (IBBR), Naples 80131, Italy

9 Department of Biology, University of Naples Federico II, Naples 80131, Italy

10 Bruker Biospin GmbH, Ettlingen 76275, Germany

11 Carl-Ludwig-Institute for Physiology, Leipzig University, Leipzig 04103, Germany

12 Euan MacDonald Centre for Motor Neurone Disease Research, University of Edinburgh, Edinburgh EH8 9AG, UK

13 Faculty of Medicine, Ottawa Hospital Research Institute, University of Ottawa, Ottawa, Ontario, K1H 8L6, Canada

14 Department of Anatomy and Cell Biology, Faculty of Medicine, Martin Luther University Halle-Wittenberg, Halle (Saale) 06108, Germany

15 Institute of Functional and Applied Anatomy, Hannover Medical School, Hannover 30625, Germany

Received March 07, 2024. Revised June 20, 2024. Accepted July 19, 2024. Advance access publication August 26, 2024

© The Author(s) 2024. Published by Oxford University Press on behalf of the Guarantors of Brain. All rights reserved. For commercial re-use, please contact reprints@oup.com for reprints and translation rights for reprints. All other permissions can be obtained through our RightsLink service via the Permissions link on the article page on our site—for further information please contact journals.permissions@oup.com.

Correspondence to: Peter Claus
 SMATHERIA gGmbH—Non-Profit Biomedical Research Institute
 Feodor-Lynen-Straße 31, Hannover 30625, Germany
 E-mail: peter.claus@smatheria.org; claus.peter@mh-hannover.de

Keywords: monogenic disease; network analysis; phosphoproteomics; translomics; metabolomics; spinal muscular atrophy

Introduction

Monogenic diseases provide the possibility to analyse molecular alterations based on loss of a single protein. These changes result in primary defects directly linked to the functions and interaction partners of the disease-causing protein. Secondary defects occur owing to dysregulation of the molecular network and homeostasis without direct connections to the mutated gene. For an optimal therapeutic impact, drugs should re-equilibrate as many alterations as possible. Therefore, it is important to identify signalling hubs and bottlenecks in the dysregulated network of primary and secondary defects, which retain the highest capacity for modulation. Hubs are nodes with a high degree of connectivity and bottlenecks are nodes in a gateway position. Both exert higher modulatory capacity in the network. In this study, we use multiple models of a monogenetic neurodegenerative and neuromuscular disease, spinal muscular atrophy (SMA), to develop a paradigm for the analysis of molecular changes caused by the loss of one protein. SMA is caused by deletion or point mutation of the survival of motor neuron 1 (SMN1) gene.¹ In humans, the SMN protein is also encoded by a second gene (SMN2) that differs from SMN1 by a critical base transition leading to alternative splicing and expression of a limited amount of functional full-length SMN. Thus, SMN2 expression fails to compensate for the loss of SMN1 in SMA patients, who show low levels of functional SMN protein.^{2,3} SMN2 copy number variation is a critical genetic modifier, with more SMN2 copies resulting in milder phenotypes.⁴ SMN is involved in basal cellular functions, such as the maturation of ribonucleoprotein (RNP) complexes,^{5,6} pre-mRNA splicing,^{7,8} regulation of the actin cytoskeleton,^{9–12} protein homeostasis¹³ or translation.^{14–17} Given that SMN is ubiquitously expressed, SMN-associated mechanisms are expected to be altered in all cells in SMA. In recent years, three therapies have been developed for SMA, all enhancing SMN expression in the nervous system and/or in the periphery.^{18–20} All treatments result in prolonged survival, but do not cure patients.²¹ Besides improvement of the neuromuscular phenotype, patients present with peripheral symptoms. SMA is now regarded as a multisystem disorder, with the need for additional treatment strategies.^{21–24}

Omics data from disease models provide information about molecular alterations at different levels of complexity. Network analysis creates a representation of the connections and dependencies between molecules. Systematic evaluation of the network structure highlights targets with high modulatory capacity upstream of pathomechanisms. In addition, data-driven approaches enable the use of such information to perform *in silico* studies for drug repurposing, minimizing the experimental and time efforts. Thus, high-quality multi-omics data are needed as a basis of disease networks. Mass spectrometry (MS)-based proteomics has been used in SMA research to identify proteins and distinct dysregulated pathways.^{25–33} SMN interactors, SMN phosphorylation, modifiers and their impact on cellular mechanisms were also studied by MS-based analysis.^{14,34–38} Although single dysregulated pathways have been identified, there is a lack of a comprehensive understanding of the main drivers in

pathobiology. A reductionistic view on specific SMN functions does not reflect the pathogenesis of the disease. Network analysis combining several omics approaches is needed to integrate the current knowledge about SMN and the mechanisms altered during SMA. Network analysis provides the opportunity to determine on a systemic level which proteins are in central positions connecting genetic cause and mechanistic outcome to target SMA.

In this study, we analysed (phospho-) proteomes of severe (FVB-Taiwanese) and less severe (BL6-*Smn*^{2B/-}) SMA mouse models to compare networks representative of different disease severities. Mice at the onset of neuronal symptomatic time points were used to identify early changes that hold the potential of being reversible upon intervention. The proteomes and phosphoproteomes were analysed to determine dysregulated pathways and their upstream regulators, including kinases. To describe SMA on a systemic level, it is necessary to link altered proteins mechanistically to the primary disease-causing protein (SMN) or to functional defects, such as translation. With this aim, we combined translome data from both mouse models at comparable time points with the proteome data. Furthermore, we performed protein–protein interaction network analyses with a focus on SMN. Thereby, model-specific entities and hubs or bottlenecks in the overarching disease network have been characterized. The identified upstream regulators, hubs and bottlenecks are most important for the understanding of the network structure behind the disease phenotypes.

This systems approach identified key modulators in the complex disease network and presented a network structure crucial to understanding all aspects of SMA pathology.

Materials and methods

Methods, including mouse models, biochemical methods, ribosome profiling, MS-based analysis, data analysis methods and an ethics statement, are included in the [Supplementary material](#).

Network construction in the Ingenuity Pathway Analysis platform and analysis of networks entities

Proteome data (P -value ≤ 0.05) from spinal cord lumbar (L)1–L5 in Taiwanese [postnatal Day (P)3] and *Smn*^{2B/-} (P12–P13) SMA mice and proxisome data from biotinylation assays in HEK293T³⁸ and NSC34 cells³⁷ were uploaded to the Ingenuity Pathway Analysis platform (IPA). Each dataset was connected by direct protein–protein interactions within the datasets and for proxisome data between proxisomes. The only interaction type selected was direct protein–protein interaction. The protein interaction databases used were IND, Cognia, DIP, MIPS, Interactome studies and Ingenuity expert information from QKB for direct interactions including different species [biomolecular interaction network database (BIND), database of interacting proteins (DIP), sequence related database (MIPS) QIAGEN knowledge base (QKB)]. The proxisome network was focused on SMN by inclusion of direct protein

connections via one additional protein (shortest path +1) to SMN. Afterwards, proteome data were connected to SMN in the same way. Non-connected nodes were deleted, and the network was exported as an undirected network to Cytoscape. In Cytoscape (v.3.10.0), the network was coloured by node border colours for datasets (blue and green). Nodes originating from several datasets (pink) and from the shortest path algorithm (grey) are also coloured. Network layout is an organic layout from yFiles representing all interactions as short connections with the least intercrossing possible. Network analysis was performed by rank-based integration of different mathematical methods from CytoHubba v.0.1.³⁹ Hubs and bottlenecks were defined by the relative ranked scoring of the top 10 nodes per method and ranked by combining their ranking in all methods relative to the number of methods used to define a hub or bottleneck. The methods used to describe different characteristics of hubs are: degree, maximal clique centrality (MCC), closeness and edge percolated component (EPC). Hubs can be in bottleneck positions, meaning that they are highly connected central nodes in a network, but also connect two or more network clusters and are therefore in restrictive regulatory positions. Bottlenecks can restrict the network paths between nodes from different clusters and are therefore in restrictive positions. Bottlenecks were defined here by the relative ranked scoring in BottleNeck, Stress and Betweenness measurements.

Statistics

Quantitative real-time (qRT)-PCR data were quantified as $\Delta\Delta C_T$ relative to housekeeping and geometric mean of intensity for data of each primer. qRT-PCR data, mouse body weights and western blot data of SMA and control samples were compared by Student's two-sided unpaired (except body weights) t-test (P -value ≤ 0.05) in GraphPad prism (v.10.1.2; ns = not significant or significant at $*P \leq 0.05$ or $**P < 0.01$). Proteome data were analysed by Student's two-sided t-test (P -value ≤ 0.05). The cut-off for Student's t-test difference for SMA versus controls was set based on the 95% confidence interval of intensities in control samples and defined as downregulated proteins < -0.2 and upregulated > 0.2 or p-sites downregulated < -0.3 and upregulated > 0.3 . Patient urine metabolites were compared with age-matched controls by the Kruskal–Wallis test for multiple comparisons (ns = not significant, adjusted P -value $*P \leq 0.05$, $**P \leq 0.01$ and $****P \leq 0.0001$). Animal numbers: proteomes, SMA $n = 5$ and control $n = 5$; phosphoproteomes, SMA $n = 5$ and control $n = 5$ (except control of Taiwanese $n = 4$ in both); translatoemes, $n = 3$.

Results

The SMA mouse models are differentially impacted by the genotypes based on proteome and phosphoproteome

In this study, we aimed to identify molecular alterations at the protein level in two SMA mouse models. We wanted to identify upstream regulators, hub and bottleneck proteins as modulatory factors of SMA, contemplate translational changes for protein alterations and describe kinases and phosphorylated target sites contributing to SMA phenotypes (Fig. 1). SMA mouse models, representative of two different severities of the disease, were analysed. SMA animals from the more severe model known as 'Taiwanese' have a lifespan until P9 on an FVB background with a knockout of *Smn1* and expression from two human SMN2 copies. The SMA animals from the less severe *Smn*^{2B/-} model have a lifespan until P25 on a BL6 background, with a

reduction of SMN expression from the murine *Smn* gene. These models were selected to reflect a broad disease spectrum with different genetic backgrounds enabling the construction of a network that highlights robust commonalities of SMA also present in these diverse genetic and developmental conditions. SMA animals showed a significant decrease in body weight compared with control littermates at the time of analysis (Supplementary Fig. 1A). In the lumbar spinal cord segments 1–5 (L1–L5) at onset of disease time points (Taiwanese at P3; *Smn*^{2B/-} at P12–P13), a depletion of SMN to 70%–80% was observed (Supplementary Fig. 1B). Sex differences and litter effects are known for SMA models.⁴⁰ Therefore, samples representative of both sexes and litter were analysed. Principal component analyses of all (Supplementary Fig. 2A–D) and significantly altered (SMA versus control; Fig. 2E–H) proteins and phosphorylation sites were performed to describe variances in the models and their impact on significant dysregulations. The most prominent component (component 1) among all quantified proteins represents the genotype for the Taiwanese model (Supplementary Fig. 2A1), whereby the *Smn*^{2B/-} model shows a strong litter component (Supplementary Fig. 2B2). Phosphoproteome data also compose the genotype as the largest component for the Taiwanese model (Supplementary Fig. 2C1); however, the *Smn*^{2B/-} model presents more components associated with litter and sex (Supplementary Fig. 2D2–3). Furthermore, component analysis of the significantly altered phosphorylation sites showed a strong litter component in the *Smn*^{2B/-} model (Supplementary Fig. 2H2). Therefore, Taiwanese model data at the onset of neuronal symptoms have a smaller impact from other factors (litter or sex) and more strongly reflect the underlying SMA genotype than the *Smn*^{2B/-} model data.

Significantly altered targets could be identified in the two SMA models

On a protein expressional level, we identified in the Taiwanese and *Smn*^{2B/-} SMA mouse models 298 of 3972 and 187 of 3522 dysregulated (P -value ≤ 0.05) proteins, respectively (Fig. 2A and Supplementary Table 1). Nine out of 46 (CNP, CPSF6, HBB-B1, SPTB, ELAVL4, PGAM, CKM, TTR and MAPK9) dysregulated proteins in the Taiwanese mice had been described in SMA. Likewise, four (ASHG, TTR, FMR1 and CPLX2) out of the 18 strongest (difference < -2 , > 2) dysregulated proteins from the *Smn*^{2B/-} mouse model are known dysregulated targets in SMA, demonstrating the validity of the experimental strategy (Supplementary Table 1, also including literature).

We aimed to describe SMA on a systems level, including changes of cellular signalling represented by specific phosphorylations compared with controls; therefore, phosphoproteomes were measured (Fig. 2B). Both phosphoproteomes comprised differentially phosphorylated sites in microtubule-associated proteins (MAP1A and MAP1B). In the phosphoproteome of the Taiwanese mice, SLC39A6 and RPS6 were strongly dephosphorylated. SLC39A6, also referred to as ZIP6/LIV-1, is a zinc transporter shifting with ZIP10 as a dimer from the endoplasmic reticulum to the cell surface upon cleavage of a PEST sequence.⁴¹ This translocation is important for mesenchymal–epithelial transition as a zinc-mediated trigger of mitosis.⁴² The p-sites (S227, T228 and S231) identified in this study are conserved in mouse and human ZIP6 and localize to the PEST site. The second prominently dephosphorylated protein was the ribosomal protein S6 (RPS6). RPS6 is part of the 40S ribosomal subunit and regulated at five p-sites (S235/36, S240/44 and S247). We found that S247, S240 and S244 were hypophosphorylated in the Taiwanese model. In the same

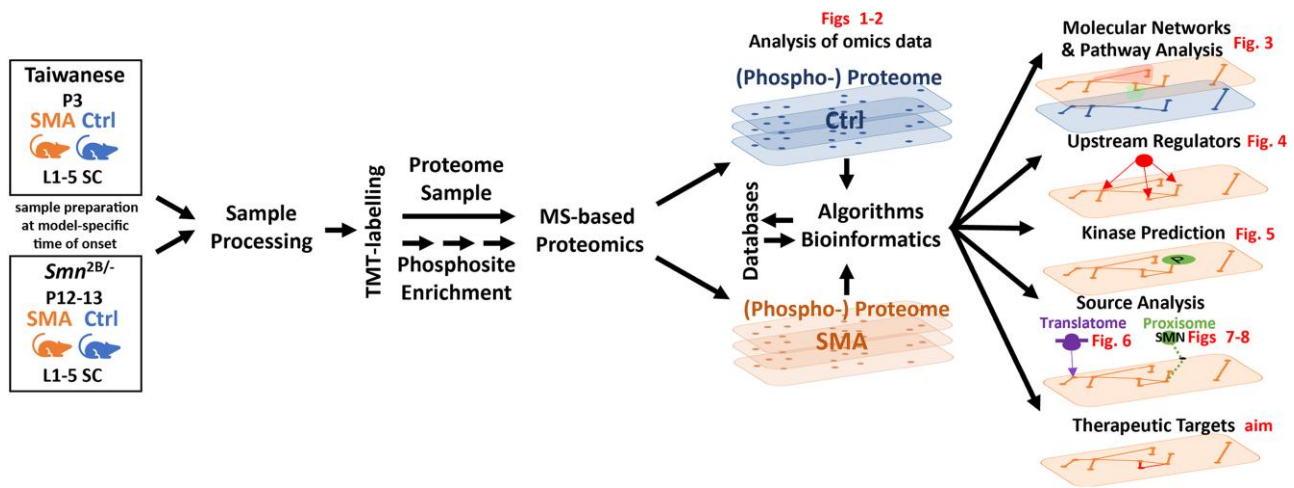


Figure 1 Experimental aim and principal components of data. Experimental scheme summarizing experimental steps, including sample selection of spinal muscular atrophy (SMA; orange) and control (Ctrl; blue) at disease onset [*Smn*^{2B/-}, postnatal Day (P)12–P13; Taiwanese, P3], processing lumbar spinal cord sections 1–5 (L1–5 SC), tandem mass tag (TMT) labelling, measurement and analysis. Experimental aims of molecular network analysis: causal analysis for alterations as SMN dependency or translational change, treatment target identification, including upstream regulators or network hubs, and kinase relationships.

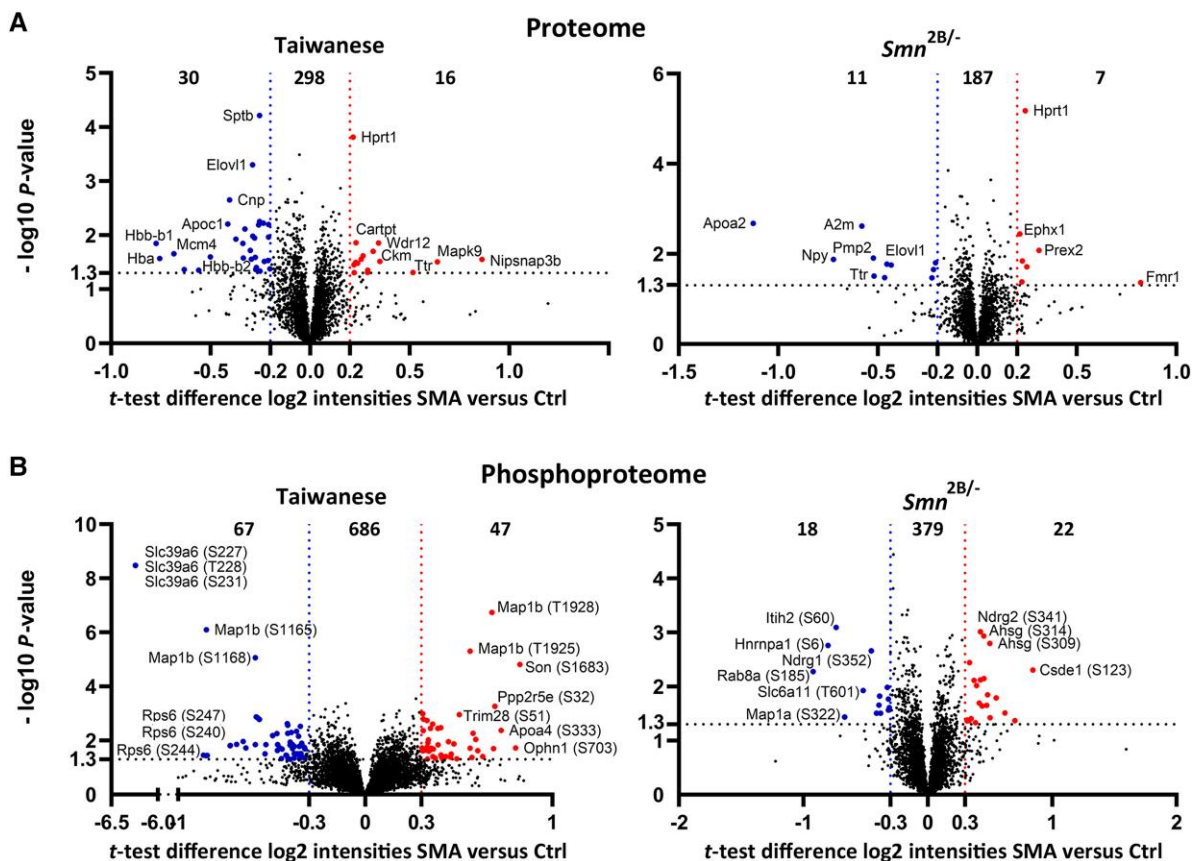


Figure 2 Volcano plots of proteome and phosphoproteome data show dysregulated proteins and p-sites. Proteins (A) and p-sites (normalized to proteins) (B) were analysed by Student's *t*-test (P -value ≤ 0.05). Cut-off for Student's *t*-test difference (calculated from \log_2 intensities, therefore equal to fold change) spinal muscular atrophy (SMA) versus control (Ctrl) was set based on the 95% confidence interval of intensity ratios from control samples and defined as downregulated proteins (< -0.2 , blue) and upregulated (> 0.2 , red) or p-sites downregulated (< -0.3 , blue) and upregulated (> 0.3 , red). Numbers of up-, down- and significantly regulated proteins and p-sites are depicted. The most strongly regulated proteins and p-sites are labelled by gene name within the plot; all other sites regulated can be taken from [Supplementary Tables 1 and 2A and B](#).

model, we confirmed by western blot analysis hypophosphorylation at S240/44 and additionally detected a hypophosphorylation at S235/36, which was not identified in the phosphoproteome analysis ([Supplementary Fig. 3](#)). Interestingly, these phosphorylations

were not significantly altered in the *Smn*^{2B/-} model ([Supplementary Fig. 4](#)). The function of RPS6 phosphorylation is still under study. S235 becomes progressively dephosphorylated during translation.⁴³ Phosphorylations at all sites depend on each

other, with phosphorylation of S235/6 being the first two and S247 the last.^{44–46} Phosphorylation at S247 enhances the affinity for the m7GpppG cap of mRNAs, linking RPS6 to translational initiation.⁴⁴

In summary, we identified alteration in expression and phosphorylation of proteins that are linked to specific disease severities, but for both models at the early onset of disease. The models differ by levels of SMN, disease onset and development⁴⁷ and are associated with distinct sets of strongly regulated proteins.⁴⁸

SMA comprises several pathomechanisms which partly overlap between models

The phenotypes and mechanisms defining SMA result from dysregulations discovered in multiple experimental systems representing different aspects of the disease. We hypothesized that models show both overlapping and model-specific mechanisms that are representative of SMA with different severities. The significantly altered proteome data from both models were analysed to identify terms describing dysregulations of functional communities in each model. Therefore, gene set enrichment analysis (GSEA) in the STRING database was used to link enriched Gene Ontology (GO) terms (BP, biological processes; MF, molecular functions; and CC, cellular compartments) in the protein networks of each model. Enriched functional terms of a protein community were highlighted in the network; colour coding depicts similar functions in both models (Fig. 3).

At a mechanistic level derived from GO terms, SMA can be described as a disease with altered splicing, including U1 snRNP binding and SMN-Sm complex assembly. Binding of RNP complexes overlaps with proteins involved in regulation of translation. Alterations affecting the ribosome were represented more prominently in the *Smn*^{2B/-} model. Fatty acid homeostasis was affected in both models, represented by different clustering GO terms in each model, whereby fatty acid beta oxidation is affected in the Taiwanese model and acetyl-CoA and cholesterol biosynthetic processes in the *Smn*^{2B/-} model. The DNA replication pathway including the methionine adenosyl transferase complex was more prominently dysregulated in the Taiwanese model. In summary, splicing was the most prominent overlapping process. Most pathways are known for SMA, whereby this approach enables the interpretation of model differences and their importance.⁴⁹ Functional clusters partly overlapped between the two models, but the regulated proteins defining those similar functions were different. Moreover, each model reflected distinct dysregulations representing different aspects of the disease. Therefore, it is likely that SMA patients display a spectrum of altered mechanisms as observed in multiple models.

To address such diverse disease aspects by common regulators, we aimed to unravel causal factors for protein and phosphorylation changes including upstream regulators and kinases. Moreover, we used data about translational changes and the interactome of SMN (proxisome) to explain network alterations mechanistically.

Upstream regulators of dysregulated proteins associated with neurodegeneration

To identify protein targets affecting both disease severities and to link them mechanistically to SMN, we analysed the overlaps between proteomes of the two mouse models. We quantified a total of 3227 of 3522 or 3972, respectively, proteins overlapping between models, demonstrating the comparability of data. Those datasets overlapped in 32 significantly regulated proteins (Fig. 4A and

Supplementary Table 1). The intersection of significantly dysregulated proteins represents a fundamental alteration because these changes are present in both models. Common changes might represent mechanisms closely connected to SMN interaction partners (proxisome).^{36,37} To test this hypothesis, we retrieved published data about SMN interaction partners derived from proximity labelling assays.^{37,38} Those assays were based on fusions of SMN with a biotin ligase, labelling all interacting proteins in the proximity of SMN with biotin; enrichment and identification were performed by mass spectrometry (Fig. 4B). We identified four proteins overlapping between models (SNRPD3, RAB21, SNRNP70 and GNAS) and interacting with SMN (Fig. 4C, pink). Interactors may overlap between models owing to mechanisms altered early in development, which are less sensitive to disease pathogenesis. GSEA showed association of overlapping proteins with small molecule metabolic processes and cholesterol/lipid/fatty acid ontologies (Fig. 4C, red).

As a next step, we compared the two models at the pathway level (IPA), thereby analysing the enrichment of significantly dysregulated proteins from the two models in functional associations and disease associations with neuronal and non-neuronal mechanisms. The first (I) analysis with the total, unbiased database [QIAGEN knowledge base (QKB)] allowed us to elucidate the general functions altered in the models (Supplementary Fig. 5A). The datasets from the two mouse models represented alterations associated with neuromuscular, movement or neurological disorders. Neuronal development, mRNA splicing and translation were functions altered in the *Smn*^{2B/-} mouse model. Microtubule, cytoskeletal organization, neurogenesis, cell viability and the formation of protrusions were altered functions in the Taiwanese mouse model. These results show that both models represent a neuronal disease with various functions being altered, but to different extents. Given that neurons often have highly specific protein expression profiles and functions, we additionally performed a second (II) canonical pathway analysis for neuronal data to gain specific results regarding the neuronal aspects of SMA (Supplementary Fig. 5B). Both datasets showed a dysregulation in cholesterol biosynthesis pathways.

Subsequently, we used our two sets of differentially expressed proteins from the two models as an input to predict upstream regulators. Those are defined as factors capable of modulating several downstream targets. Upstream regulators are putatively efficient treatment targets. We combined upstream regulator analysis of both proteomes to identify regulators upstream to at least four dysregulated targets from each model (Fig. 4D). The prediction included information about the activity of putative upstream regulators being either inactivated in SMA (Fig. 4D, blue) or activated (Fig. 4D, red). Regulatory factors overlapping between models were HTT, MAPT, MTOR, APP, PSEN1 and SOD1, which are known to play a role in neurodegenerative diseases.^{50,51} Inactivated upstream regulators predicted for both datasets were SH3TC2, TARDBP (TDP-43), BDNF and EGR2. Those are also associated with neurological diseases.^{50,52,53} Upon activation, these regulators potentially rescue mechanisms altered in neurological diseases.

Distinct kinases are related to dysregulated phospho-sites in both SMA models

Expression analysis lacks the information about post-translational modifications on proteins. Phosphorylations, regulated by kinases and phosphatases, are important post-translational modifications controlling pathway responses to alterations of cellular

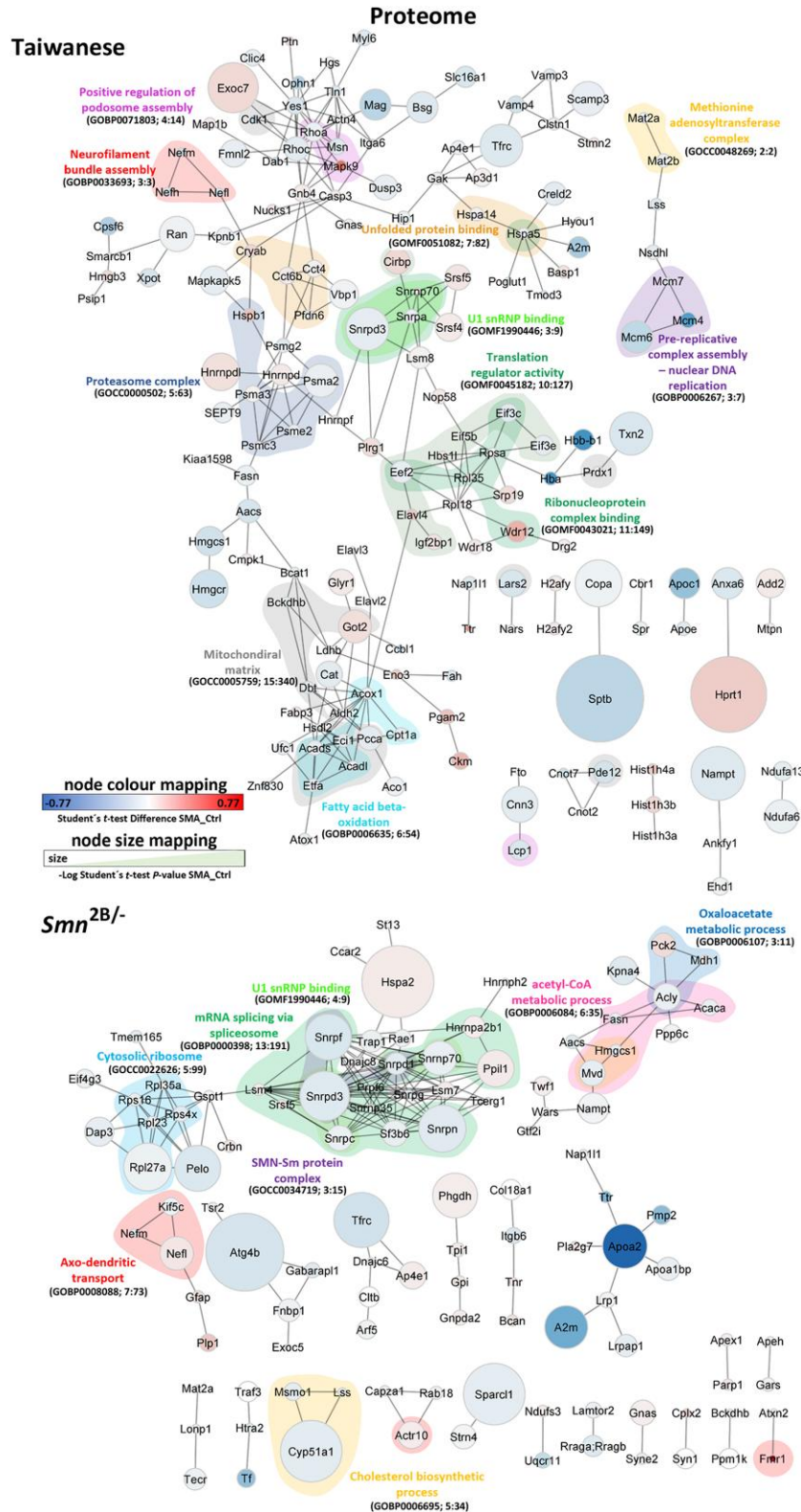


Figure 3 Gene set enrichment analysis on protein association networks. Proteins dysregulated in Taiwanese and *Smn*^{2B/-} spinal muscular atrophy (SMA) data (lumbar spinal cord 1–5) are connected by database and experimental information in STRING DB (v.12.0), shown as undirected lines in networks. Unconnected dysregulated proteins are not shown. Enriched associated Gene Ontology (GO) terms were overlaid, and those clustering on connected proteins are displayed as coloured underlining. Term names, unique identifiers and overlap size are depicted. Similar GO terms are displayed in similar colours. Node size is correlated with $-\text{Log Student's } t\text{-test } P\text{-value}$ from proteome data. Node colour is correlated with $t\text{-test}$ difference of data (blue, downregulated, < -0.2 ; red, upregulated, > 0.2 ; continuous colouring).

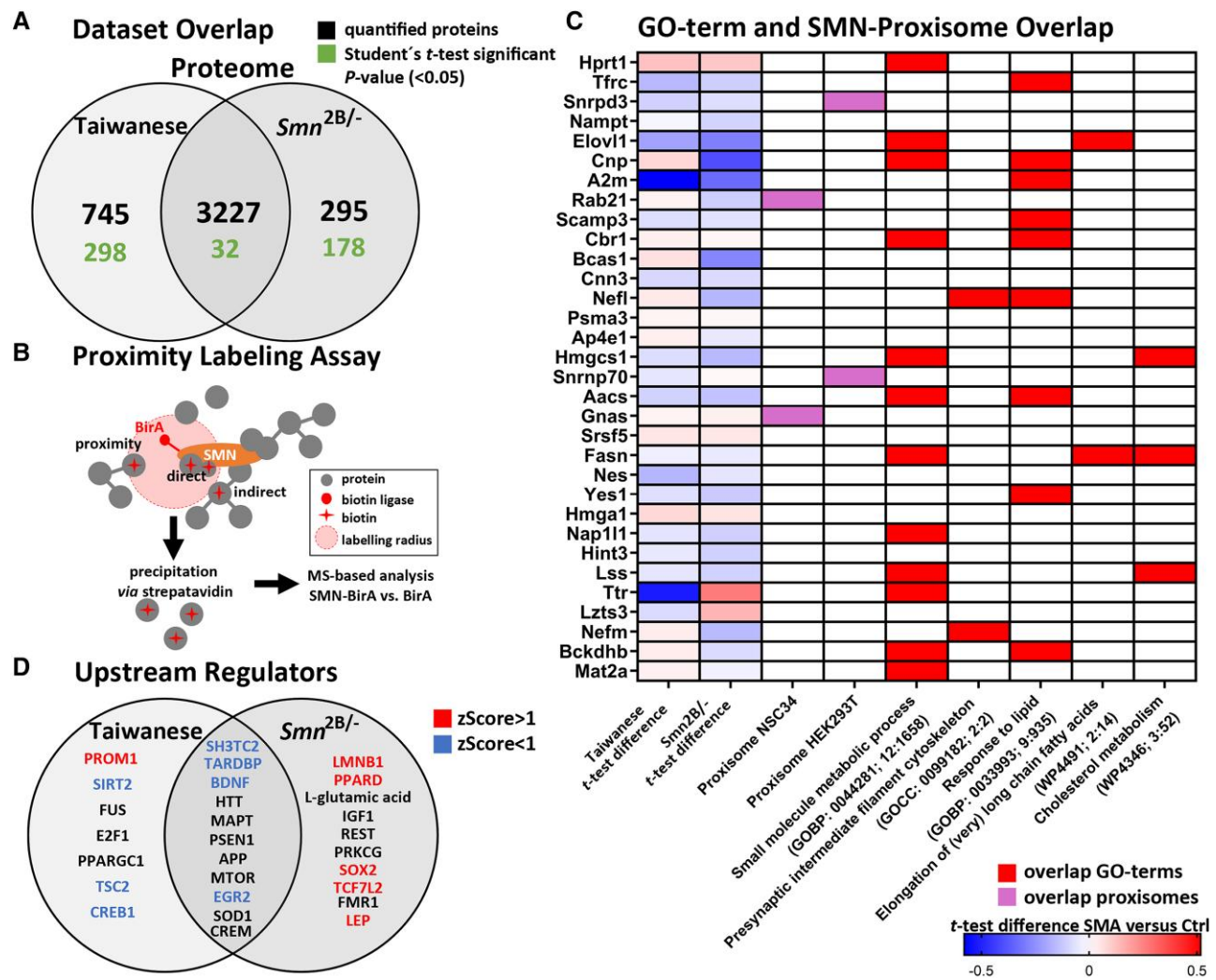


Figure 4 Model overlapping targets and upstream regulators. (A) Venn diagram of proteins that could be quantified by mass spectrometry (MS; black) and those that are significantly different between spinal muscular atrophy (SMA) and control (Student's t-test P -value ≤ 0.05 , green) significant proteins. (B) Scheme representing a proximity labelling assay used to generate SMN-proxisome data. Proxisome data included in this study are from public data.^{37,38} Proximity labelling was performed in NSC34 or HEK293T cells, whereby the biotin ligase BirA (red) fused to the bait protein SMN (orange) was used. Within a defined labelling radius, proteins of proximity, including direct and indirect interactors, were labelled covalently by biotin ligation. After cell lysis, biotinylated proteins were immunoprecipitated and identified by MS-based proteomics. (C) Heat map of the 32 overlapping significantly regulated proteins of proteome data from SMA mouse models (sorted by the average of P -values from Taiwanese and $Smn^{2B/-}$ data; P -value ≤ 0.05). The first two columns show Student's t-test differences based on \log_2 intensities and are therefore fold changes, SMA versus control (Ctrl), of proteome data (blue, decreased in SMA; red, increased in SMA). The third and fourth lanes show the overlap with SMN-proxisome datasets (pink), and the last lanes show the association of five Gene Ontology (GO) terms enriched on proteins taken from String DB (GO term ID and node size overlap in brackets, red). Details on proteins are included in [Supplementary Table 1](#). (D) Venn diagram of upstream regulators targeting at least four dysregulated proteins from both proteome datasets. Analysis was made on neuronal data in the QIAGEN knowledge base (QKB). Ingenuity pathway analysis (IPA) z-scores for predicted inhibition (blue) and activation (red) are included (black indicates opposite z-scores or no z-score predicted).

homeostasis. In a similar manner to the elucidation of upstream regulators, we identified upstream kinases based on the dysregulated sites found in the SMA phosphoproteomes. Twenty-two sites of the altered phosphoproteins overlapped (Fig. 5A and [Supplementary Table 2](#)), whereas 355 or 662 sites, respectively, were model specific. We used the analysis pipeline PhosR to identify kinases related to altered p-sites.⁵⁴ First, the variability of phosphorylation between samples was normalized to a set of known consistent phosphorylation sites called 'stably phosphorylated sites'.⁵⁴ Kinases responsible for phosphorylation of specific sites were identified by information from the database PhosphositePlus, kinase recognition motifs and the dynamic

phosphorylation profiles of sites between samples. Kinases were ranked by the combined scores across these databases.⁵⁴ The resulting scores represent the probability of each kinase to regulate a site. To illustrate the associated p-sites for each kinase, the top three p-sites per kinase are shown with the corresponding association scores in a heat map including hierarchical clustering (Fig. 5B and C). These sites did not overlap between the mouse models, but associated kinases showed similarities. Kinases are classified in groups by the substrate they act on, and groups are split into families. Kinases that were putatively responsible for alterations of p-sites in SMA map to kinase groups and families (Fig. 5B and C). Nine kinases overlapped between models (AURKB,

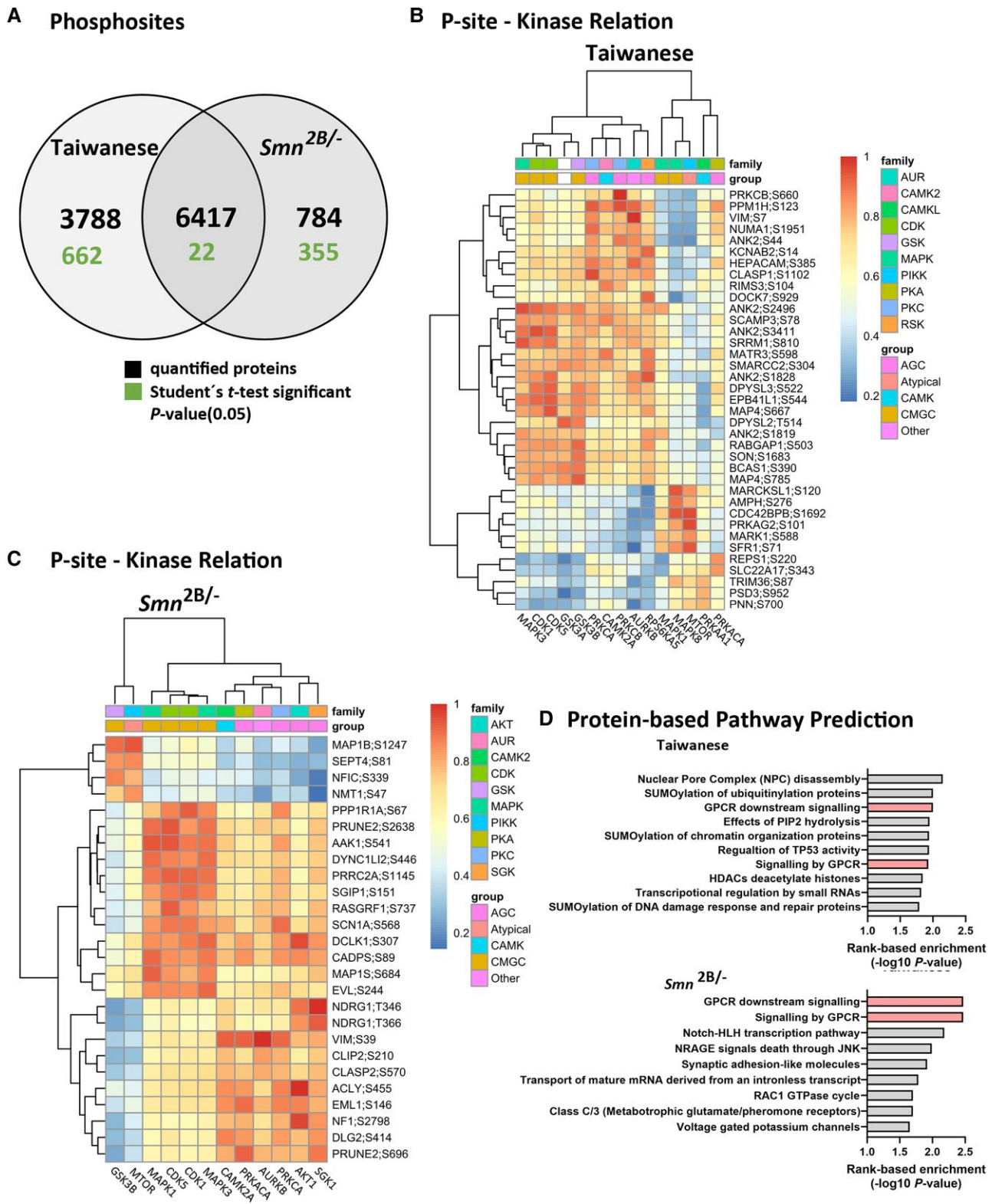


Figure 5 Phosphorylation site (p-site)–kinase relationships and dysregulated pathways based on phosphoproteins. (A) Venn diagram of all p-sites that could be quantified by mass spectrometry (MS; black) and those that are significantly different between spinal muscular atrophy (SMA) and control (Student's *t*-test *P*-value ≤ 0.05 , green) significant p-sites. (B and C) Heat maps summarizing the top three dysregulated p-sites per associated kinase. Colour code represents association probability with increasing probability [blue (low, 0.2) to red (high, 1)]. Kinase–site associations are predicted by PhosR based on knowledge from the database PhosphositePlus, kinase recognition motifs and the dynamic phosphorylation profiles of sites between samples. Hierarchical clustering represents site and kinase associations, whereby kinase associations are correlated in part with kinase families and groups. (D) Top 10 ($-\log_{10}$ *P*-value) signalling pathways predicted to be dysregulated based on Taiwanese and Smn^{2B/-} phosphoproteome data. Prediction was performed based on PhosR protein-centric analysis. Model overlapping pathways are coloured in red.

PRKACA, CAMK2A, MAPK3, MAPK1, CDK1, CDK5, MTOR and GSK3B). MTOR, GSK3B, CDK5 and MAPK are already known to be associated with SMA.^{51,55–58} Those kinases associated with dysregulated p-sites are putatively altered in their activities. Second, we elucidated the signalling pathways represented by phosphorylation changes, as potential mechanisms of SMA pathogenesis. We performed protein-centric analyses, in which a dysregulated site was interpreted as a dysregulation of the protein itself, therefore lacking information regarding additional sites on this protein. Gene sets were ranked by classical enrichment analysis on pathways (Fig. 5D). G-protein coupled receptor (GPCR) downstream signalling was altered in both mouse models. In conclusion, the identified kinases represent regulators with potentially high modulatory capacity on the disease, similar to upstream regulators. However, the analyses of signalling also revealed several pathways that are selectively dysfunctional in either the Taiwanese or the *Smn*^{2B/-} mouse model. The data demonstrate that the disease is functionally distinct in the two mouse models of SMA, with different aspects in pathomechanisms of SMA and external factors interfering with those.

Translation accounts for single protein alterations and resembles mechanisms observed in proteomes

Translation plays a crucial role in SMA, and translation of several mRNAs is known to be affected owing to SMN deficiency in the severe Taiwanese mouse model.^{14,15} These transcripts, also known as SMN-specific mRNAs, are involved in multiple cellular processes and pathways. Here, we hypothesize that translational changes overlap with dysregulated proteomes, thereby possibly accounting for alterations in proteomes. Hence, to identify transcripts showing alterations in ribosome occupancy, we performed ribosome profiling of whole spinal cords in both the Taiwanese and *Smn*^{2B/-} models of SMA at similar stages used for previous proteome analysis (Taiwanese, P3; *Smn*^{2B/-}, P10). After differential expression analysis, we found 126 and 295 mRNAs with changes in ribosome occupancy in the Taiwanese and *Smn*^{2B/-} mice, respectively. By GSEA, we found that these mRNAs are associated with functional communities that are associated with chromosomes, translation, splicing, mRNA processing and cytoskeletal organization (Fig. 6A). These functional communities are similar to those identified in the proteome analysis, e.g. with regard to translation, pre-mRNA splicing and RNA regulation (Fig. 3). For a systematic comparison, we combined translomes and proteomes (Fig. 6B) and found two model-specific proteins that are altered at both omics levels [RhoA and Dlgap4 (Taiwanese); and Syn1 and Rps4x (*Smn*^{2B/-})]. Synapsin 1 (Syn1) was the only protein regulated with a coherent direction of changes in both proteome and translome analysis (Fig. 6C). Syn1 coats synaptic vesicles and binds the cytoskeleton, regulating vesicle trafficking.⁵⁹ We analysed overlaps between translomes and proteomes mechanistically in both models by GSEA (Fig. 6D). Interestingly, we identified enriched GO terms (synapse, spliceosomal snRNP complex, myelin sheath and melanosome), which include proteins from both omics levels. Specifically, Myelin sheath proteins are known to exhibit reduced protein expression owing to perturbations in protein translation in primary Schwann cells expressing low levels of SMN protein from the Taiwanese model.⁶⁰ These findings suggest that some dysregulations in proteomes are linked to translational alterations in SMA. The consensus in dysregulation might increase by aligning technical differences between both methods, such as performing ribosome profiling from lumbar spinal cord. The overlap of data reflects that additional mechanistic

changes might be responsible for downstream changes in protein levels, such as protein degradation.¹³

The SMA–SMN network: HSPA5 and HSPB5 are bottleneck proteins linking SMN and SMA

The proteomic alterations are partly linked to translational changes. Another critical and proximate cause for alterations is the lost interactions of SMN and the functions of those interacting partners. However, the link between the genetic cause and phenotypes in SMA remains inconclusive without considering network properties. SMN interacts with many proteins and affects several fundamental pathways. Here, we combined interactomics with the proteome data to elucidate the causal relationship between loss of a protein, as in SMA as a monogenic disease, and protein changes. We used the information from two SMN-proxisome datasets to identify mechanistic links between SMN and dysregulated proteins (Supplementary Table 3).^{37,38} We calculated a protein–protein interaction (PPI) network based on direct protein interactions only. The two SMN-proxisomes used comprised 287 (analysed in motor neuron-like NSC34 cells) and 147 (analysed in human embryonic kidney HEK293T cells) proteins, respectively. Twelve proteins are shared between the two datasets (GIGYF1, TDRD3, GEMIN8, G3BP2, SNRPD2, SNRPA, EIF4ENIF1, PLATL1, FOCAD, TOP3B, LSM14A and ITPA) and SMN itself owing to its ability to oligomerize. To calculate a comprehensive protein interaction network of SMN, we first connected SMN-proxisomes by direct PPI within and then between each other (Fig. 7A). Proteins that do not directly bind to SMN might be indirect interactors via a bridging protein. Therefore, we connected those by a shortest path algorithm via PPI (Fig. 7A, via dark green +1). This step included 26 additional proteins (grey nodes in Fig. 7B). Proteins or small clusters of proteins from the SMN-proxisome data that did not connect to the SMN network are not displayed. The resulting SMN network was used to identify direct PPI to proteomic data from the SMA models. To identify SMN-dependent nodes, SMA proteomes (Fig. 7A and Supplementary Table 4) were connected to SMN via the SMN-proxisome network by shortest path algorithm accepting one additional protein to connect to SMN via PPI. This step used several proxisome proteins already present in the network and introduced three additional proteins to the network to connect the dysregulation to SMN (Fig. 7A and grey nodes in Fig. 7B). The network was arranged by a force-directed layout, whereby SMN shows up centred as the genetic cause of the disease (Fig. 7B).

The network represents information about the systemic nature of SMA. Nodes in critical positions are potential targets to address this disease network most efficiently. Network analysis was performed by rank-based integration of different mathematical methods in CytoHubba.³⁹ Hubs, which are nodes in central positions, were defined by the relative ranked scoring in degree, maximal clique centrality, closeness and edge percolated component. Bottlenecks, which are nodes in key gateway positions, were defined by the relative rank scoring in BottleNeck, Stress and Betweenness measurements. Hubs are highly connected centred proteins (orange). Bottleneck hubs (red) are highly connected and in a gateway position on network paths between nodes. Non-hub bottlenecks (yellow) are between clusters in the network and therefore are key connector proteins.⁶¹ As expected, the most central bottleneck hub is SMN, because inclusion of SMN interactions from proxisome data biased the network. The bottleneck hubs GRB2, EGFR, TP53 and BCL2 in the SMA network are proteins included by the shortest path method. FUS, AGO2, HTT and SMN

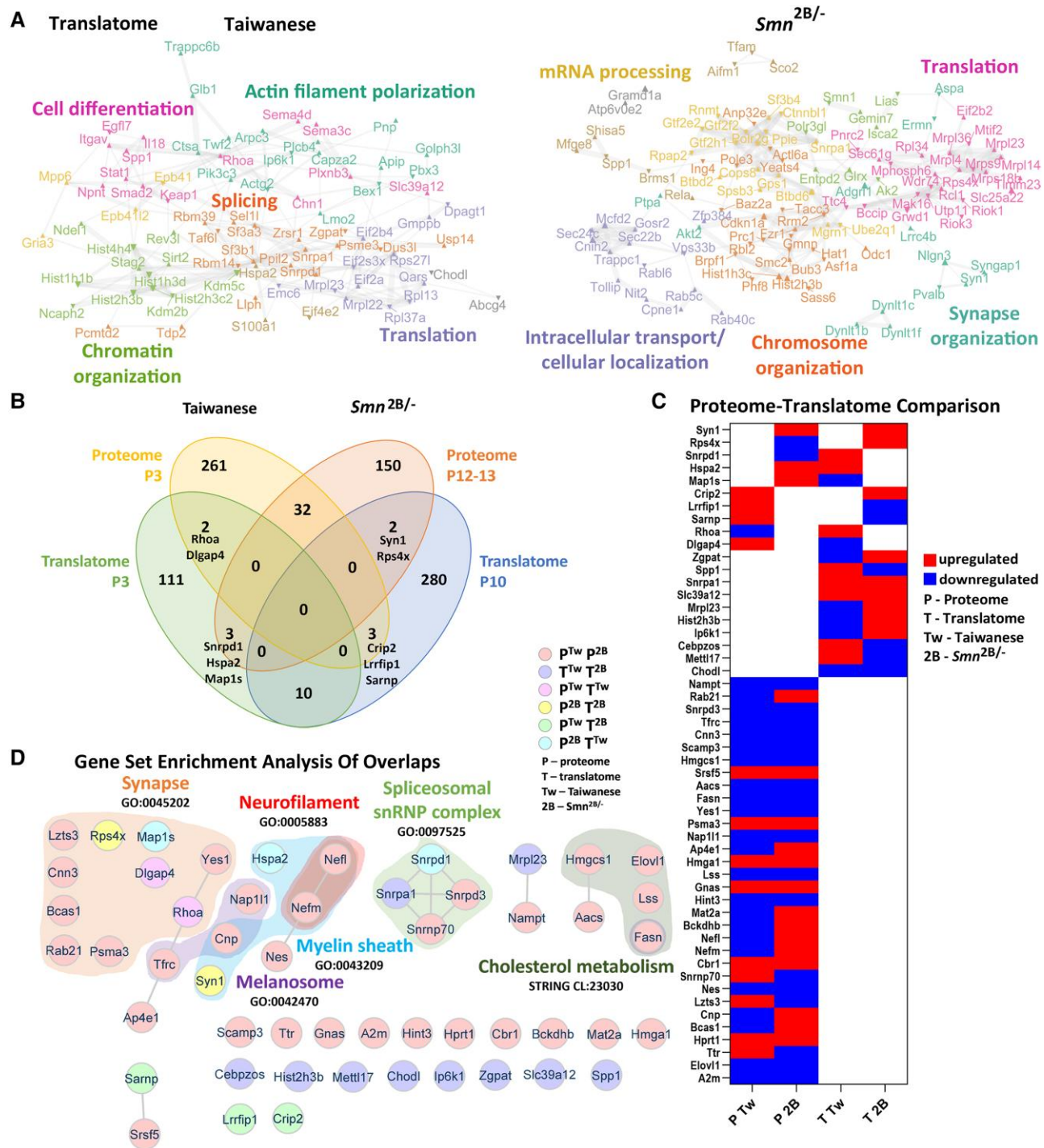


Figure 6 Protein-protein interaction network on transcripts with altered ribosome occupancy in the Taiwanese and *Smn*^{2B/-} mouse models and proteome-translatome comparisons. Ribosomal activity as a potential cause of protein expression changes. (A) Ribosome profiling sequencing data of total spinal cord samples from the Taiwanese [postnatal Day (P)3, n = 3; transcripts, n = 6115] and *Smn*^{2B/-} (P10, n = 3; transcripts, n = 7234) mice were analysed to determine alterations in protein-coding transcript translation. Transcripts showing significantly altered ribosome occupancy [P-value ≤ 0.05, fold change (FC) ± 0.3] were analysed by protein-protein interaction and gene set enrichment analysis. Communities enriched in genes are highlighted for each model. (B) Venn diagram of protein overlaps between significantly altered proteins [P-value ≤ 0.05, translatome: log₂ fold change (log₂ FC) ± 0.3, proteome: t-test difference of log₂ ± 0.3]. (C) Heat map of overlapping proteins sorted by datasets (P = proteome; T = translatome; Tw = Taiwanese; 2B = *Smn*^{2B/-}). Colour coding refers to upregulation (red, translatome P-value ≤ 0.05, log₂ FC > 0.3, proteome P-value ≤ 0.05, difference positive) or downregulation (blue) owing to different fold-change scales in different methods. (D) Protein-protein interaction network (experimental and database information from STRING DB, confidence > 0.4) and gene set enrichment analysis of overlapping proteins with highlighted GO terms and STRING clusters. Colours of nodes refer to datasets whereby P = proteome, T = translatome, Tw = taiwanese, and 2B = *Smn*^{2B/-}.

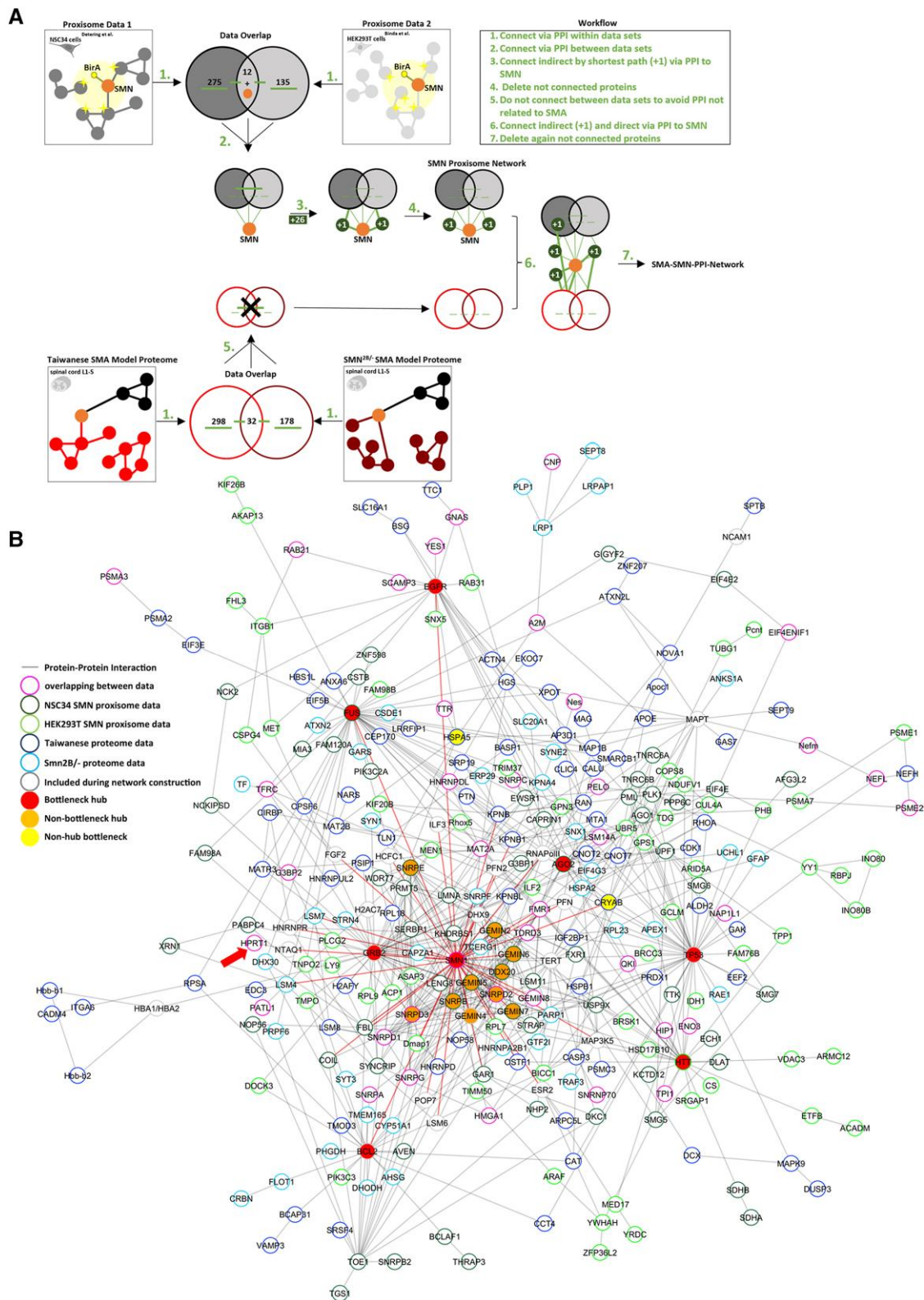


Figure 7 Protein–protein interaction (PPI) network of SMN-proximosome and proteome data: SMN interaction as source of protein dysregulation. (A) Workflow of data processing and PPI inclusion. Proximosome data (Fig 4B) represent proteins biotinylated (yellow cross represents biotin) by biotin ligase BirA-SMN (yellow-orange) construct expressed in murine NSC34 cells³⁷ and human HEK293T cells.³⁸ Direct and indirect interactors within the radius of the ligase (yellow circle) are included in data. Upper Venn diagram displays proximosome data overlap. First, direct PPI between proteins within one dataset were included in the network. PPI are displayed as thick green lines when added in that step and as thin green lines in previous steps. Next, PPI between

(Continued)

are bottleneck hubs included in SMN-proxisome data. The identified hubs connect the genetic cause with mechanistic dysregulations from the proteome data. Network analysis revealed two bottleneck nodes: heat shock protein family A (Hsp70) member 5 (HSPA5, also named BiP) and alpha-crystallin B chain (CRYAB, also named HSPB5) (yellow nodes). Both were dysregulated (P -value ≤ 0.05 , difference not significantly changed) in the Taiwanese SMA mouse model, whereby western blot analysis showed no significant alteration (Supplementary Fig. 6A). But both proteins were downregulated at the transcript level in SMA mice from the Taiwanese model at P3 in qRT-PCR (Supplementary Fig. 6B). Given that bottlenecks are in critical regulatory positions of a network, these proteins might be key to maintain molecular homeostasis in SMA. Taken together, we developed a PPI network representative for SMN-dependent dysregulation in SMA models. Network analysis revealed several hub proteins and HSPA and HSPB5 at bottleneck positions (Supplementary Table 5), which represent potential treatment targets for SMA at a systemic level.

HPRT upregulation and hypoxanthine increase in SMA type I imply the power of network analysis to focus research

Unexpectedly, hypoxanthine-guanine-phosphoribosyltransferase (HPRT) was the strongest (P -value) upregulated protein of both SMA models (Fig. 2). Even more surprisingly, the SMA-SMN network shows a close connection of HPRT to SMN via one additional node [N-terminal glutamine amidase 1 (NTAQ1)] previously identified in a PPI network project⁴⁷ (Fig. 7B). HPRT is an enzyme involved in recycling of guanine and hypoxanthine in the purine salvage pathway (Fig. 8A). We confirmed the protein increase by western blot analysis of spinal cord lysates at P3 in the Taiwanese model (Fig. 8B). Furthermore, the levels of *Hprt* transcript were upregulated in the Taiwanese SMA model at P3 and P5 in qRT-PCR (Fig. 8C). This makes *Hprt* a non-suitable gene for normalization, because it is frequently used for this in quantitative PCR.⁶² From these results, we hypothesize that HPRT might have a role in metabolic pathomechanisms in SMA patients. We reanalysed ¹H NMR data from urine including only treatment-naïve patients with an age <1 year, representing a relatively homogeneous cohort.⁶³ We evaluated creatinine, xanthine and hypoxanthine levels in symptomatic patients with SMA type I, presymptomatic patients from newborn screening (NBS) and healthy age-matched controls (Fig. 8D). Hypoxanthine normalized to creatinine was upregulated in SMA type I and presymptomatic patients (Fig. 8D). Xanthine was also significantly increased in presymptomatic patients. Type I patients did not show a significant increase, probably owing to a smaller group size. A mechanistic connection of urine metabolites in patients to increased HPRT levels in murine spinal cord cannot

be drawn, but this could predict energy demand on the systemic level. This is supported by the finding that *Hprt* transcript levels tended to be increased in lung and kidney from Taiwanese SMA mice at P3 and kidney from *Smn*^{2B/-} mice (Supplementary Fig. 6C). Thus, we show the importance of unbiased network biology approaches to understand the systemic connectivity of SMA, enabling the development of new research questions to target SMA most efficiently.

Discussion

Mutations or deletions of the *SMN1* gene, leading to low levels of SMN protein, are the monogenic cause of SMA. The molecular links to pathomechanisms and phenotypes are largely unknown. SMN affects basal cellular functions, such as the maturation of RNP complexes,^{5,6} pre-mRNA splicing,^{7,8} protein homeostasis,¹³ translation¹⁴⁻¹⁷ or regulation of the actin cytoskeleton.⁹⁻¹² The current approved treatments increase SMN levels and lead to significant improvements in the disease, but they do not cure SMA. Here, we used network biology to provide valuable insights into the pathomechanisms of SMA and their connection to SMN. By proteome and phosphoproteome analysis, the aim of this study was to identify molecular alterations at the protein and signalling levels and to predict key proteins and kinases involved in SMA. The combination of two animal models with different genetic backgrounds aimed to reflect the broad disease spectrum from mild to more severe and different developmental stages also given in patients. Therefore, an overlap in data and mechanisms can be assumed as a fundamental aspect of the disease. Furthermore, we combined translomes and SMN-proxisome data to identify mechanisms of protein dysregulation for an improved understanding of SMA.

In the phosphoproteome, ribosomal protein S6 (RPS6), a structural component of the small ribosomal subunit 40S, was differentially phosphorylated at all five functional sites (S235/36, S240/44 and S247) in the Taiwanese mouse model. The mechanisms of phosphorylation at these five p-sites have not yet been determined in detail. These sites are phosphorylated and dephosphorylated during ribosomal assembly and translational control of gene expression.^{44,64} Thereby, the kinase S6K is upstream of all p-sites, with S240/44 being phosphorylated exclusively by this enzyme.⁶⁵ mTOR and ERK signalling are the two main pathways upstream of RPS6 phosphorylation, with ERK regulating primarily S235/36. In SMA, BRAF activity was shown to be decreased, and ERK increased presumably as a compensational effect through a crosstalk with increased ROCK signalling in lumbar spinal cord of symptomatic (P6) Taiwanese mice.^{56,66} ERK does not directly phosphorylate RPS6, and a regulation by the intermediate kinase RSK2 could limit its activity

Figure 7 Continued

proxisomes were included. To connect proteins interacting indirectly with SMN as included in proxisomes, single (+1) proteins interconnecting via PPI were added. This shortest path method added 26 proteins not included in the datasets. After removal of non-connected proteins, the SMN-proxisome network is completed. Proteome data from Taiwanese and *Smn*^{2B/-} SMA mice are loaded to be included next (red). Proteomes may overlap in dysregulated proteins (black) and include model-specific dysregulated proteins (light and dark red). Lower Venn diagram represents proteome data overlap. First PPI within data were added to the network of proteome data. To identify SMN-connected proteins, the proteome data were connected to the SMN-proxisome network by the shortest path (+1 protein) PPI to SMN, whereby three new proteins were added. Final removal of non-connected proteins results in the SMA-SMN PPI network in (B). Nodes represent proteins from proxisome and proteome data with gene names annotated in capital letters because human and murine data are included. The network is constructed in Cytoscape in yFiles-organic layout. The border colours of nodes represent datasets [pink, overlapping in several datasets (details in Supplementary Table 4); dark green, NSC34 proxisome; light green, HEK293T proxisome; dark blue, proteome of Taiwanese SMA mice; light blue, proteome of *Smn*^{2B/-} SMA mice; grey, included during shortest path finding]. Hubs and bottlenecks were defined by combination of different network descriptive models (Supplementary Table 5): red, non-bottleneck hubs; orange, bottleneck hubs; and yellow, non-hub bottlenecks. Interacting proteins are also listed in Supplementary Table 4.

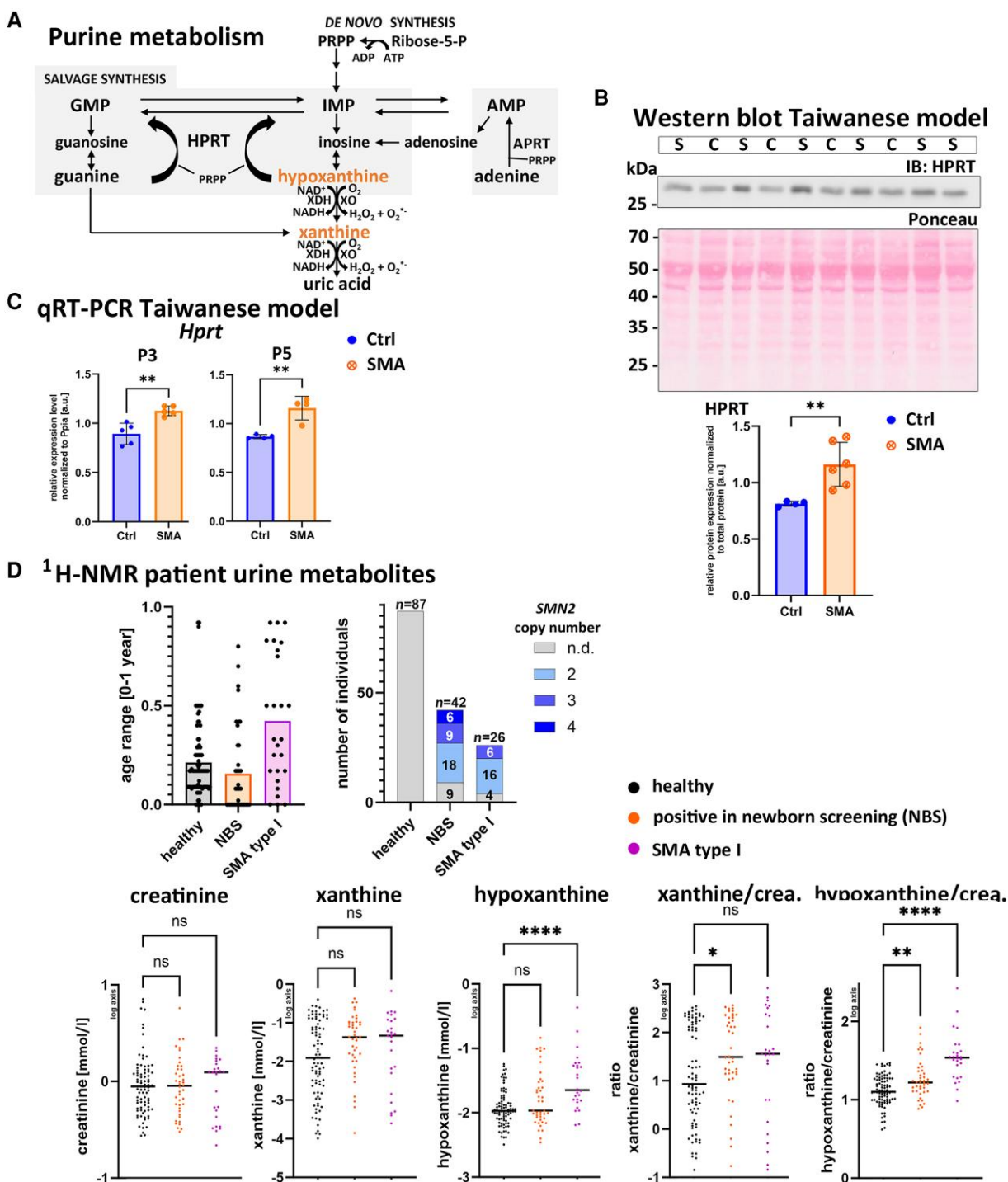


Figure 8 Salvage pathway dysregulation in spinal muscular atrophy (SMA). (A) Schematic representation of the purine metabolism, including *de novo* synthesis and the salvage pathway. APRT = adenosine phosphoribosyltransferase; GMP/IMP/AMP = guanosine/inosine/adenosine monophosphate; HPRT = hypoxanthine phosphoribosyltransferase; PRPP = α -5'-phosphoribosyl-1'-pyrophosphate; XDH = xanthine dehydrogenase; XO = xanthine oxidase; orange, measured metabolites in patients. (B) Western blot of lumbar (L) L1–L5 spinal cord lysates from control (C, blue, $n = 4$) and SMA (S, orange, $n = 6$) animals from the Taiwanese mouse model at postnatal day (P)3. Total protein was stained with Ponceau S for quantification. Student's *t*-test, SMA versus control (Ctrl), with P -value ≤ 0.05 , ** $P < 0.01$. (C) Quantitative real-time (qRT)-PCR of L1–L5 spinal cord from the Taiwanese mouse model. Postnatal Day (P)3 animals are $n = 5$ from three litters; P5 animals are $n = 4$ from two litters. Mean C_T values from duplicates of *Hprt* were normalized to mean C_T values from triplicates of *Ppia*, normalized to the geometric mean of *Hprt* primer intensity and inverted for display. Student's *t*-test with $P \leq 0.05$ was used, ** $P \leq 0.01$. (D) Urine metabolites measured by ¹H NMR from patients and healthy controls. Bar graphs summarize the analysed groups, with healthy age-matched samples, samples from presymptomatic patients from newborn screening (NBS), and symptomatic SMA type I patients. The first graph includes the age range (in years). The second graph represents the SMN2 copy numbers (n.d. = not determined) from each individual (increasing copy number by increasing darkness of blue colour). Bottom graphs depict metabolites, including creatinine, xanthine and hypoxanthine (in millimoles per litre), and their ratios (black, healthy; orange, newborn screening; purple, SMA type I; \log_{10} axis). Kruskal–Wallis test for multiple comparisons was used, comparing patients with healthy controls (ns = not significant, adjusted P -value * $P \leq 0.05$, ** $P \leq 0.01$ and **** $P \leq 0.0001$).

towards this target.^{65,67} In addition, several other kinases can phosphorylate S235/6.⁶⁵ Loss of phosphorylation on RPS6 might affect translation efficiency of several mRNAs.⁴³ In SMA, translational defects were shown *in vivo* and *in vitro*, which are cell autonomous and SMN dependent.¹⁵ Therefore, the identified p-sites might be important for regulating the translational role of SMN.

Comparison of datasets between mouse models identified overlapping proteins that are in proximity to SMN. One of these interaction partners is RAB21, a small GTPase and part of the proxisome of SMN in murine motor neuron-like NSC34 cells.³⁷ RAB21 associates with integrin and regulates endosome formation and endosomal trafficking.⁶⁸ In addition, small nuclear ribonucleoprotein D3 polypeptide (SNRPD3) and small nuclear ribonucleoprotein U1 subunit 70 (SNRPD70) were dysregulated in the proxisome of HEK293T cells.³⁸ SNRPD3 is a direct interaction partner of SMN in the assembling of U1, U2, U4 and U5 snRNAs.⁶⁹ SNRPD70 is necessary for gem integrity and binds to the SMN complex.⁷⁰ G-protein alpha isoform short (GNAS) is also in proximity to SMN, and G-protein-coupled receptor signalling was found to be dysregulated based on the phosphoproteome data from both mouse models. How this dysregulation contributes to the pathomechanisms needs to be studied in more detail in order to differentiate GDP/GTP-bound G-protein and its location to SMN.

The pathway analysis also revealed upstream regulators that are putative therapeutic targets. Identified upstream regulators of protein alterations in both models exert functions in other neurological diseases. Predicted upstream regulators of differentially phosphorylated proteins were the kinases MTOR, GSK3 and MAPK previously linked to SMA.^{11,51,55} To evaluate whether the dysregulation of proteins results from translational changes, translome data from both models were compared with proteomes. Significantly dysregulated proteins and protein-coding transcripts overlapped for 10 proteins. This set belongs to synaptic, spliceosomal snRNP and myelin sheath gene ontologies. Those protein alterations might be a result of translational changes early in pathogenesis. We hypothesize that protein alterations are partly impacted by decreased recruitment of ribosomes to polysomes owing to loss of SMN. Nonetheless, the low correlation of translomes and proteomes highlights that on both biological levels mechanisms are altered, but most are not directly traceable over several biological levels.

The PPI network focused on SMN provides a framework for the understanding of molecular communities in SMA and SMN-dependent dysregulations. The identification of hub and bottleneck proteins within this network is instrumental to define therapeutic targets that could be used in combinatorial therapies. The discovery of bottleneck hub proteins found in the SMN-proxisome data, such as FUS, AGO2, HTT and SMN itself, underscores their central roles in SMA pathology. As expected by the network construction focusing on SMN, the hubs identified connect SMN and other proteins in central positions, whereby all are part of the SMN–snRNP complex. This accumulation of hubs originating from both proteome data and included during network construction highlights the commonality between models and proxisomes in this central function of SMN acting in snRNP assembly. Given that all hubs are closely related in one function, they might present redundant targets to modulate the disease in this mechanical aspect. HSPA5 and CRYAB (also named HSPB5) are two heat shock proteins identified here as bottleneck factors. Those might be critical for maintaining molecular homeostasis in SMA.^{71–73} HSPA5 (also named GRP78, BiP) is an endoplasmic reticulum chaperone and a regulator of protein folding.⁷² In addition, HSPA5 binds to 'AGAG' motifs regulating 5'UTR alternative splicing in non-

alcoholic fatty liver disease.⁷⁴ Interestingly, this disease has been described as a peripheral defect in SMA.⁷⁵ The second identified bottleneck, CRYAB (HSPB5), is part of the small heat shock protein (sHSP) family with an ATP-independent function regulating protein aggregation.⁷³ CRYAB interacts directly with SMN and is imported upon phosphorylation to the nucleus by the SMN complex, where it localizes to nuclear speckles and mitotic interchromatin granules.⁷¹ Both proteins present only a minor fold change in proteomes and are not significantly altered when analysed by western blot, representing their low dependency on expressional level to SMN. The high connection within the network reflects a potential to address SMA pathomechanisms via these proteins. Transcript levels were altered at P3 in the Taiwanese model, underlining their association with SMA. Phosphorylation on identified phosphorylation sites from the Taiwanese model is not altered (not identified in *Smn*^{2B/-} mice). Heat shock protein regulation is a rapid and tightly regulated process upon environmental change. Therefore, protein and transcript alteration might be detectable only by analysing kinetics or by sensitive methods. The capacity as a treatment option needs to be studied in more detail.⁷⁶ In particular, extracellular heat shock proteins are involved in disease mechanisms modulating immune responses. Extracellular CRYAB and BiP are regulators in inflammatory conditions, such as in EAE mice, a model for multiple sclerosis or rheumatoid arthritis, respectively.^{59,77} In SMA, heat shock proteins have a modulatory capacity, as shown by a variant of the chaperone HSPA8 identified to influence SNARE complex assembly and improve SMA phenotypes.⁷⁸

In this study, HPRT was identified to be upregulated at both protein (Taiwanese and *Smn*^{2B/-} mice) and transcriptional (Taiwanese P3, P5) levels. Unexpectedly, in the SMA-SMN network, HPRT connects via one additional protein by direct protein–protein interactions to SMN.⁴⁷ HPRT is a ribosyltransferase in the salvage pathway for recycling purines with lower energy demand than by *de novo* synthesis. Alterations of energy supply are linked to SMA by different means. Our data show downregulation of NAMPT, a central enzyme in NAD⁺ salvage synthesis and changes in mitochondrial and metabolic proteins.⁷⁹ Interestingly, we could identify dysregulations in the salvage pathway metabolism by ¹H NMR analysis of patient urine. Symptomatic SMA type I patients and presymptomatic patients from newborn screening showed an increase in hypoxanthine, a substrate of HPRT, compared with age-matched controls. Xanthine, the downstream product of hypoxanthine and guanine, was also increased in presymptomatic samples. The analysed patient groups were restricted by age (<1 year), and only treatment-naïve samples were considered, representing a cohort informative for metabolic alterations based on SMA pathomechanisms. Another study identified a decreased abundance of xanthine and hypoxanthine in urine of highly symptomatic children with SMA, possibly resulting from nutrition differences.⁸⁰ Here, we compared infants younger than 1 year and observed an increase of those metabolites before onset of symptoms. An increase in excretion of purines, such as adenine, was identified in children with different neuromuscular disorders.⁸¹ A decrease of adenine nucleotide was observed in atrophic muscles, probably resulting from an increased nucleotide degradation.⁸² In summary, purine metabolic alterations might result from nucleotide degradation and energy homeostatic changes. Inhibition of degradation of xanthine via xanthine oxidoreductase (XO) inhibitors in a mouse model for amyotrophic lateral sclerosis delayed disease progression.⁸³ We suggest that HPRT plays a role in SMA pathomechanisms on a systemic level, which might depend closely on SMN, as shown in the network analysis.

Conclusion

The identification of several proteins, kinases, signalling pathways and potential therapeutic targets highlights the complexity of this monogenic disease and the need for combinatorial approaches for treatment. The findings provide a solid foundation for future research aimed at developing effective therapies for SMA, complementing the current therapies on a systemic level. SMA is a multisystem disease, hence equivalent data and network approaches are needed for peripheral tissues at different disease stages. These will highlight key functions common between cell types and organs. The analysis of this study is a paradigm for elucidating relevant regulators of molecular pathomechanisms in monogenic diseases. Key for understanding systemic relationships is the combination of different omics types representing signalling, translation and interacting protein partners.

Data availability

All datasets can be provided by the corresponding author on request. The SMA-SMN network was saved on NDEX v.2.5.6 and can be viewed at: <https://doi.org/10.18119/N9T020>.

Acknowledgements

We acknowledge the NCT Cell and Liquid Biobank, a member of BioMaterialBank Heidelberg, for providing and processing patient urine samples for ¹H NMR spectroscopy. We thank all patients and families for participation in this study. We thank our colleagues from the collaborating centres in Munich (Professor Dr W. Mueller-Felber and A. Blaschek) and Hamburg (Dr J. Johannsen) for collecting and sending the patient samples. For technical support within ribosome profiling experiments, we acknowledge the staff at the Core Facilities Next Generation Sequencing (NGS) Facility and High Throughput Screening (HTS) at Department CIBIO, University of Trento, Italy.

Funding

This project was funded by the Deutsche Muskelstiftung (DMS) (to SMATHERIA gGmbH—Non-Profit Biomedical Research Institute, Hannover, Germany) and SMA Europe (project SMATARGET to N.H., E.D.S. and P.C.). This work was also supported by the European Union's Horizon 2020 research and innovation program (project SMABEYOND, No. 956185). Ribosome profiling was supported by: AFM Telethon (#23692); Telethon (GGP19115 and GMR23T1048); and EU funding within the MUR PNRR 'National Center for Gene Therapy and Drugs based on RNA Technology' (Project no. CN00000041 CN3 RNA). ¹H NMR spectroscopy analysis of urine samples was supported within a Sponsor research agreement with Biogen Inc. (project MetabSMA to A.Z., No. GER-SPN-19-11493) and within a funding from the Dietmar-Hopp-Foundation, St. Leon-Rot, Germany (project INSPECTOR, No. 1DH2011115).

Competing interests

The authors report no competing interests. A.Z. and P.C. received honoraria for presentations and advisory boards from Biogen, Avexis (to A.Z.), Novartis and Roche, outside of the submitted work.

Supplementary material

Supplementary material is available at *Brain* online.

References

- Lefebvre S, Bürglen L, Reboullet S, et al. Identification and characterization of a spinal muscular atrophy-determining gene. *Cell*. 1995;80:155-165.
- Vitte J, Fassier C, Tiziano FD, et al. Refined characterization of the expression and stability of the SMN gene products. *Am J Pathol*. 2007;171:1269-1280.
- Lorson CL, Hahnen E, Androphy EJ, Wirth B. A single nucleotide in the SMN gene regulates splicing and is responsible for spinal muscular atrophy. *Proc Natl Acad Sci U S A*. 1999;96:6307-6311.
- Ogino S, Gao S, Leonard DGB, Paessler M, Wilson RB. Inverse correlation between SMN1 and SMN2 copy numbers: Evidence for gene conversion from SMN2 to SMN1. *Eur J Hum Genet*. 2003;11:275-277.
- Young PJ, Le TT, Dunckley M, thi Man N, Burghes AHM, Morris GE. Nuclear gems and Cajal (coiled) bodies in fetal tissues: Nucleolar distribution of the spinal muscular atrophy protein, SMN. *Exp Cell Res*. 2001;265:252-261.
- Young PJ, Le TT, thi Man N, Burghes AHM, Morris GE. The relationship between SMN, the spinal muscular atrophy protein, and nuclear coiled bodies in differentiated tissues and cultured cells. *Exp Cell Res*. 2000;256:365-374.
- Meister G. SMN-mediated assembly of RNPs: A complex story. *Trends Cell Biol*. 2002;12:472-478.
- Pellizzoni L. Chaperoning ribonucleoprotein biogenesis in health and disease. *EMBO Rep*. 2007;8:340-345.
- Giesemann T, Rathke-Hartlieb S, Rothkegel M, et al. A role for polyproline motifs in the spinal muscular atrophy protein SMN. *J Biol Chem*. 1999;274:37908-37914.
- Rademacher S, Verheijen BM, Hensel N, et al. Metalloprotease-mediated cleavage of PlexinD1 and its sequestration to actin rods in the motoneuron disease spinal muscular atrophy (SMA). *Hum Mol Genet*. 2017;26:3946-3959.
- Hensel N, Rademacher S, Claus P. Chatting with the neighbors: Crosstalk between rho-kinase (ROCK) and other signaling pathways for treatment of neurological disorders. *Front Neurosci*. 2015;9:198.
- Nölle A, Zeug A, van Bergeijk J, et al. The spinal muscular atrophy disease protein SMN is linked to the rho-kinase pathway via profilin. *Hum Mol Genet*. 2011;20:4865-4878.
- Chaytow H, Huang YT, Gillingwater TH, Faller KME. The role of survival motor neuron protein (SMN) in protein homeostasis. *Cell Mol Life Sci*. 2018;75:3877-3894.
- Lauria F, Bernabò P, Tebaldi T, et al. SMN-primed ribosomes modulate the translation of transcripts related to spinal muscular atrophy. *Nat Cell Biol*. 2020;22:1239-1251.
- Bernabò P, Tebaldi T, Groen EJM, et al. *In vivo* translome profiling in spinal muscular atrophy reveals a role for SMN protein in ribosome biology. *Cell Rep*. 2017;21:953-965.
- Deng C, Reinhard S, Hennlein L, et al. Impaired dynamic interaction of axonal endoplasmic reticulum and ribosomes contributes to defective stimulus-response in spinal muscular atrophy. *Transl Neurodegener*. 2022;11:31.
- Béchade C, Rostaing P, Cisterni C, et al. Subcellular distribution of survival motor neuron (SMN) protein: Possible involvement in nucleocytoplasmic and dendritic transport. *Eur J Neurosci*. 1999;11:293-304.
- Mendell JR, Al-Zaidy S, Shell R, et al. Single-dose gene-replacement therapy for spinal muscular atrophy. *N Engl J Med*. 2017;377:1713-1722.

19. Sturm S, Günther A, Jaber B, et al. A phase 1 healthy male volunteer single escalating dose study of the pharmacokinetics and pharmacodynamics of risdiplam (RG7916, RO7034067), a SMN2 splicing modifier. *Br J Clin Pharmacol*. 2019;85:181-193.
20. Chiriboga CA, Swoboda KJ, Darras BT, et al. Results from a phase 1 study of nusinersen (ISIS-SMN₂) in children with spinal muscular atrophy. *Neurology*. 2016;86:890-897.
21. Motyl AAL, Faller KME, Groen EJM, et al. Pre-natal manifestation of systemic developmental abnormalities in spinal muscular atrophy. *Hum Mol Genet*. 2020;29:2674-2683.
22. Hensel N, Kubinski S, Claus P. The need for SMN-independent treatments of spinal muscular atrophy (SMA) to complement SMN-enhancing drugs. *Front Neurol*. 2020;11:45.
23. Hamilton G, Gillingwater TH. Spinal muscular atrophy: Going beyond the motor neuron. *Trends Mol Med*. 2013;19:40-50.
24. Shababi M, Lorson CL, Rudnik-Schöneborn SS. Spinal muscular atrophy: A motor neuron disorder or a multi-organ disease? *J Anat*. 2014;224:15-28.
25. Roberto J, Poulin KL, Parks RJ, Vacratsis PO. Label-free quantitative proteomic analysis of extracellular vesicles released from fibroblasts derived from patients with spinal muscular atrophy. *Proteomics*. 2021;21:2000301.
26. Šolčić D, Shorrock HK, Allardyce H, et al. Lamin A/C dysregulation contributes to cardiac pathology in a mouse model of severe spinal muscular atrophy. *Hum Mol Genet*. 2019;28:3515-3527.
27. Eshraghi M, Gombar R, De Repentigny Y, Vacratsis PO, Kothary R. Pathologic alterations in the proteome of synaptosomes from a mouse model of spinal muscular atrophy. *J Proteome Res*. 2019;18:3042-3051.
28. Varderidou-Minasian S, Verheijen BM, Harschnitz O, et al. Spinal muscular atrophy patient iPSC-derived motor neurons display altered proteomes at early stages of differentiation. *ACS Omega*. 2021;6:35375-35388.
29. Meijboom KE, Webber C, Bowerman M, et al. Combining multiomics and drug perturbation profiles to identify muscle-specific treatments for spinal muscular atrophy. *JCI Insight*. 2021;6:e149446.
30. Kobayashi DT, Shi J, Stephen L, et al. SMA-MAP: A plasma protein panel for spinal muscular atrophy. *PLoS One*. 2013;8:e60113.
31. Fuller HR, Mandefro B, Shirran SL, et al. Spinal muscular atrophy patient iPSC-derived motor neurons have reduced expression of proteins important in neuronal development. *Front Cell Neurosci*. 2016;9:506.
32. Aghamaleky Sarvestany A, Hunter G, Tavendale A, et al. Label-free quantitative proteomic profiling identifies disruption of ubiquitin homeostasis as a key driver of Schwann cell defects in spinal muscular atrophy. *J Proteome Res*. 2014;13:4546-4557.
33. Mutsaers CA, Lamont DJ, Hunter G, Wishart TM, Gillingwater TH. Label-free proteomics identifies Calreticulin and GRP75/Mortalin as peripherally accessible protein biomarkers for spinal muscular atrophy. *Genome Med*. 2013;5:95.
34. Sivaramakrishnan M, McCarthy KD, Campagne S, et al. Binding to SMN2 pre-mRNA-protein complex elicits specificity for small molecule splicing modifiers. *Nat Commun*. 2017;8:1476.
35. Walter LM, Rademacher S, Pich A, Claus P. Profilin2 regulates actin rod assembly in neuronal cells. *Sci Rep*. 2021;11:10287.
36. Wen HL, Lin YT, Ting CH, Lin-Chao S, Li H, Hsieh-Li HM. Stathmin, a microtubule-destabilizing protein, is dysregulated in spinal muscular atrophy. *Hum Mol Genet*. 2010;19:1766-1778.
37. Detering NT. Posttranslational modifications of the spinal muscular atrophy gene product SMN: Implications for therapy and pathophysiology. Thesis. University of Veterinary Medicine Hannover; 2021. https://elib.tiho-hannover.de/receive/tiho_mods_00005981
38. Binda O, Juillard F, Ducassou JN, et al. SMA-linked SMN mutants prevent phase separation properties and SMN interactions with FMRP family members. *Life Sci Alliance*. 2023;6:e202201429.
39. Chin CH, Chen SH, Wu HH, Ho CW, Ko MT, Lin CY. cytoHubba: Identifying hub objects and sub-networks from complex interactome. *BMC Syst Biol*. 2014;8(S4):S11.
40. Laird AS, Mackovski N, Rinkwitz S, Becker TS, Giacomotto J. Tissue-specific models of spinal muscular atrophy confirm a critical role of SMN in motor neurons from embryonic to adult stages. *Hum Mol Genet*. 2016;25:1728-1738.
41. Hogstrand C, Kille P, Ackland ML, Hiscox S, Taylor KM. A mechanism for epithelial-mesenchymal transition and anoikis resistance in breast cancer triggered by zinc channel ZIP6 and STAT3 (signal transducer and activator of transcription 3). *Biochem J*. 2013;455:229-237.
42. Nimmanon T, Ziliotto S, Ogle O, et al. The ZIP6/ZIP10 heteromer is essential for the zinc-mediated trigger of mitosis. *Cell Mol Life Sci*. 2021;78:1781-1798.
43. Bohlen J, Roiuk M, Teleman AA. Phosphorylation of ribosomal protein S6 differentially affects mRNA translation based on ORF length. *Nucleic Acids Res*. 2021;49:13062-13074.
44. Hutchinson JA, Shanware NP, Chang H, Tibbetts RS. Regulation of ribosomal protein S6 phosphorylation by casein kinase 1 and protein phosphatase 1. *J Biol Chem*. 2011;286:8688-8696.
45. Martin-Pérez J, Thomas G. Ordered phosphorylation of 40S ribosomal protein S6 after serum stimulation of quiescent 3T3 cells. *Proc Natl Acad Sci U S A*. 1983;80:926-930.
46. Wettenhall RE, Erikson E, Maller JL. Ordered multisite phosphorylation of *Xenopus* ribosomal protein S6 by S6 kinase II. *J Biol Chem*. 1992;267:9021-9027.
47. Rual JF, Venkatesan K, Hao T, et al. Towards a proteome-scale map of the human protein-protein interaction network. *Nature*. 2005;437:1173-1178.
48. Jablonka S, Sendtner M. Developmental regulation of SMN expression: Pathophysiological implications and perspectives for therapy development in spinal muscular atrophy. *Gene Ther*. 2017;24:506-513.
49. Singh RN, Howell MD, Ottesen EW, Singh NN. Diverse role of survival motor neuron protein. *Biochim Biophys Acta Gene Regul Mech*. 2017;1860:299-315.
50. Giau V, Senanarong V, Bagyinszky E, An S, Kim S. Analysis of 50 neurodegenerative genes in clinically diagnosed early-onset Alzheimer's disease. *Int J Mol Sci*. 2019;20:1514.
51. Rehorst WA, Thelen MP, Nolte H, et al. Muscle regulates mTOR dependent axonal local translation in motor neurons via CTRP3 secretion: Implications for a neuromuscular disorder, spinal muscular atrophy. *Acta Neuropathol Commun*. 2019;7:154.
52. Okamoto Y, Takashima H. The current state of Charcot-Marie-Tooth disease treatment. *Genes (Basel)*. 2023;14:1391.
53. Ibrahim AM, Chauhan L, Bhardwaj A, et al. Brain-derived neurotrophic factor in neurodegenerative disorders. *Biomedicines*. 2022;10:1143.
54. Kim HJ, Kim T, Hoffman NJ, et al. Phosr enables processing and functional analysis of phosphoproteomic data. *Cell Rep*. 2021;34:108771.
55. Sansa A, Miralles MP, Beltran M, et al. ERK MAPK signaling pathway inhibition as a potential target to prevent autophagy alterations in spinal muscular atrophy motoneurons. *Cell Death Discov*. 2023;9:113.
56. Hensel N, Cieri F, Santonicola P, et al. Impairment of the neurotrophic signaling hub B-Raf contributes to motoneuron degeneration in spinal muscular atrophy. *Proc Natl Acad Sci U S A*. 2021;118:e2007785118.

57. Genabai NK, Ahmad S, Zhang Z, Jiang X, Gabaldon CA, Gangwani L. Genetic inhibition of JNK3 ameliorates spinal muscular atrophy. *Hum Mol Genet.* 2015;24:6986-7004.
58. Miller N, Xu Z, Quinlan KA, et al. Mitigating aberrant Cdk5 activation alleviates mitochondrial defects and motor neuron disease symptoms in spinal muscular atrophy. *Proc Natl Acad Sci U S A.* 2023;120:e2300308120.
59. Panayi GS, Corrigan VM. Immunoglobulin heavy-chain-binding protein (BiP): A stress protein that has the potential to be a novel therapy for rheumatoid arthritis. *Biochem Soc Trans.* 2014;42:1752-1755.
60. Hunter G, Sarvestany AA, Roche SL, Symes RC, Gillingwater TH. SMN-dependent intrinsic defects in Schwann cells in mouse models of spinal muscular atrophy. *Hum Mol Genet.* 2014;23:2235-2250.
61. Yu H, Kim PM, Sprecher E, Trifonov V, Gerstein M. The importance of bottlenecks in protein networks: Correlation with gene essentiality and expression dynamics. *PLoS Comput Biol.* 2007;3:e59.
62. Townsend MH, Felsted AM, Ence ZE, et al. Falling from grace: HPRT is not suitable as an endogenous control for cancer-related studies. *Mol Cell Oncol.* 2019;6:1575691.
63. Saffari A, Cannet C, Blaschek A, et al. ¹H-NMR-based metabolic profiling identifies non-invasive diagnostic and predictive urinary fingerprints in 5q spinal muscular atrophy. *Orphanet J Rare Dis.* 2021;16:441.
64. James A, Wang Y, Raje H, Rosby R, DiMario P. Nucleolar stress with and without p53. *Nucleus.* 2014;5:402-426.
65. Biever A, Valjent E, Puighermanal E. Ribosomal protein S6 phosphorylation in the nervous system: From regulation to function. *Front Mol Neurosci.* 2015;8:75.
66. Hensel N, Baskal S, Walter LM, Brinkmann H, Gernert M, Claus P. ERK and ROCK functionally interact in a signaling network that is compensationally upregulated in spinal muscular atrophy. *Neurobiol Dis.* 2017;108(September):352-361.
67. Roux PP, Shahbazian D, Vu H, et al. RAS/ERK signaling promotes site-specific ribosomal protein S6 phosphorylation via RSK and stimulates cap-dependent translation. *J Biol Chem.* 2007;282:14056-14064.
68. Jean S, Cox S, Nassari S, Kiger AA. Starvation-induced MTMR 13 and RAB 21 activity regulates VAMP 8 to promote autophagosome-lysosome fusion. *EMBO Rep.* 2015;16:297-311.
69. Jodelka FM, Ebert AD, Duelli DM, Hastings ML. A feedback loop regulates splicing of the spinal muscular atrophy-modifying gene, SMN2. *Hum Mol Genet.* 2010;19:4906-4917.
70. Stejskalová E, Staněk D. Splicing factor U1-70K interacts with the SMN complex and is required for nuclear Gem integrity. *J Cell Sci.* 2014;127:3909-15.
71. Sarparanta J, Jonson PH, Kawan S, Udd B. Neuromuscular diseases due to chaperone mutations: A review and some new results. *Int J Mol Sci.* 2020;21:1409.
72. Radons J. The human HSP70 family of chaperones: Where do we stand? *Cell Stress Chaperones* 2016;21:379-404.
73. Janowska MK, Baughman HER, Woods CN, Klevit RE. Mechanisms of small heat shock proteins. *Cold Spring Harb Perspect Biol.* 2019;11:a034025.
74. Rehati A, Abuduaini B, Liang Z, Chen D, He F. Identification of heat shock protein family A member 5 (HSPA5) targets involved in nonalcoholic fatty liver disease. *Genes Immun.* 2023;24:124-129.
75. Deguise M, Baranello G, Mastella C, et al. Abnormal fatty acid metabolism is a core component of spinal muscular atrophy. *Ann Clin Transl Neurol.* 2019;6:1519-1532.
76. Alagar Boopathy LR, Jacob-Tomas S, Alecki C, Vera M. Mechanisms tailoring the expression of heat shock proteins to proteostasis challenges. *J Biol Chem.* 2022;298:101796.
77. Guo Y-S, Liang P-Z, Lu S-Z, Chen R, Yin Y-Q, Zhou J-W. Extracellular α B-crystallin modulates the inflammatory responses. *Biochem Biophys Res Commun.* 2019;508:282-288.
78. Kim JK, Jha NN, Awano T, et al. A spinal muscular atrophy modifier implicates the SMN protein in SNARE complex assembly at neuromuscular synapses. *Neuron.* 2023;111:1423-1439.e4.
79. Thelen MP, Wirth B, Kye MJ. Mitochondrial defects in the respiratory complex I contribute to impaired translational initiation via ROS and energy homeostasis in SMA motor neurons. *Acta Neuropathol Commun.* 2020;8:223.
80. Finkel RS, Crawford TO, Swoboda KJ, et al. Candidate proteins, metabolites and transcripts in the biomarkers for spinal muscular atrophy (BforSMA) clinical study. *PLoS One.* 2012;7:e35462.
81. Bertorini TE, Palmieri GMA, Airozo D, Edwards NL, Fox IH. Increased adenine nucleotide turnover in Duchenne muscular dystrophy. *Pediatr Res.* 1981;15:1478-1482.
82. Miller SG, Hafen PS, Brault JJ. Increased adenine nucleotide degradation in skeletal muscle atrophy. *Int J Mol Sci.* 2019;21:88.
83. Kato S, Kato M, Kusano T, Nishino T. New strategy that delays progression of amyotrophic lateral sclerosis in G1H-G93A transgenic mice: Oral administration of xanthine oxidoreductase inhibitors that are not substrates for the purine salvage pathway. *J Neuropathol Exp Neurol.* 2016;75:1124-1144.